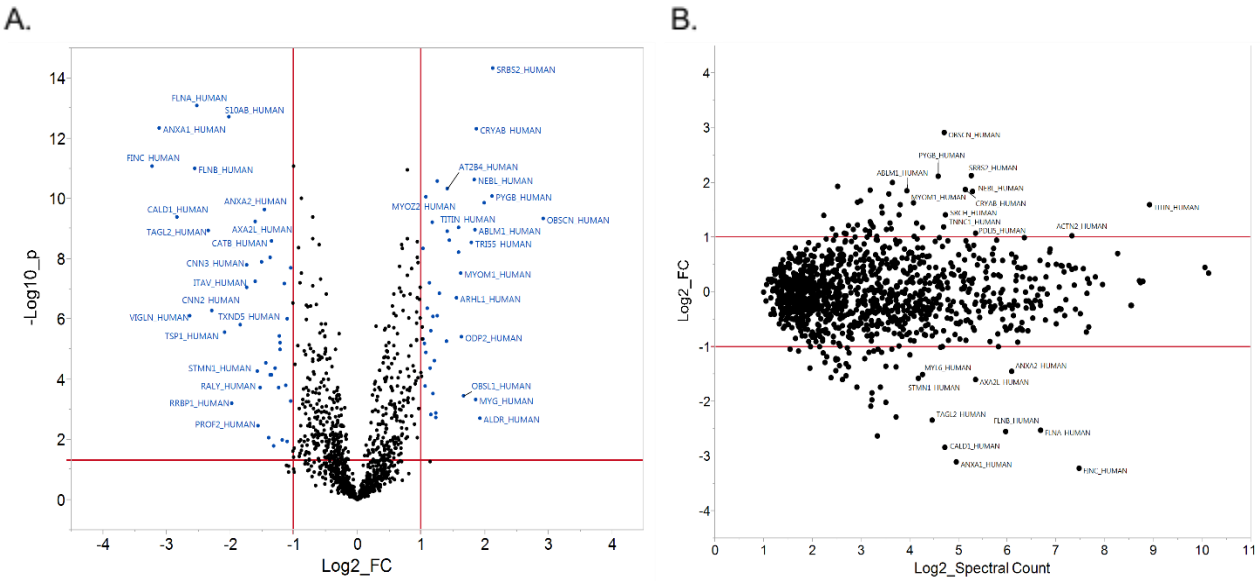

Supplementary Figure 1. Overview over proteomic profiles of WT vs. OGFOD1-KO cardiomyocytes. A) Volcano plot to compare the mean $\log_2$ fold-change (KO/WT) of normalized spectral counts and the $\log_{10}$ of the p-values. Protein classes are highlighted and annotated for proteins with a fold increase of > 2. The horizontal line represents the threshold of p=0.05, and the vertical lines represent the threshold for the $\log_2$ fold-changes. The x-axis depicts the $\log_2$ difference in protein level. B) Av plot showing the $\log_2$ spectral count values in relation to the $\log_2$ fold changes (KO/WT) which gives an impression about overall abundance of the protein classes. High abundant proteins with differences in levels between KO and WT are annotated. The horizontal line represents the false positive control (FDR) at 1%, the vertical lines represent the threshold for the $\log_2$ fold-change ($\log_2$FC). The x-axis depicts the $\log_2$ difference in estimated abundance values.

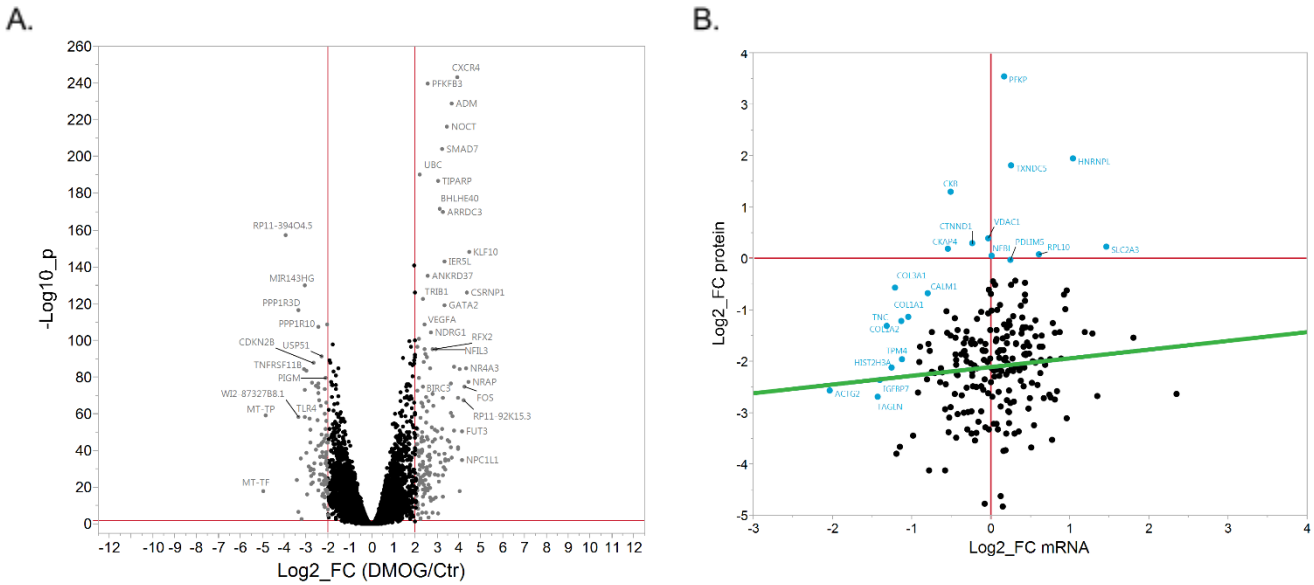

Supplementary Figure 2. Cardiac transcriptomes obtained by RNA-sequencing and correlation to protein translation shown for the effect of DMOG in WT. A) Volcano plot shows RNA-sequencing data in DMOG-treated WT cardiomyocytes vs. Ctr. The horizontal line represents the false positive control (FDR) at 1%, the vertical lines represent the threshold for the $\log_2$ fold-changes ($\log_2$FC). The x-axis depicts the $\log_2$ difference in estimated relative expression values. Vertical lines represent the threshold for the $\log_2$ fold change. Transcripts up-regulated (right) or down-regulated (left) which are changed greater than 4-fold are highlighted in grey. B) Correlation of mRNA with protein synthesis of the effect of DMOG in WT. The red lines highlight the zero value, the green line shows the fit between $\log_2$ fold changes in mRNA levels (x-axis) and the $\log_2$ fold changes in protein synthesis (y-axis). The horizontal line represents the false positive control (FDR) at 1%, the vertical lines represent the threshold for the $\log_2$ fold-change ($\log_2$FC). Targets in blue represent a good correlation between protein synthesis and changes in mRNA levels.

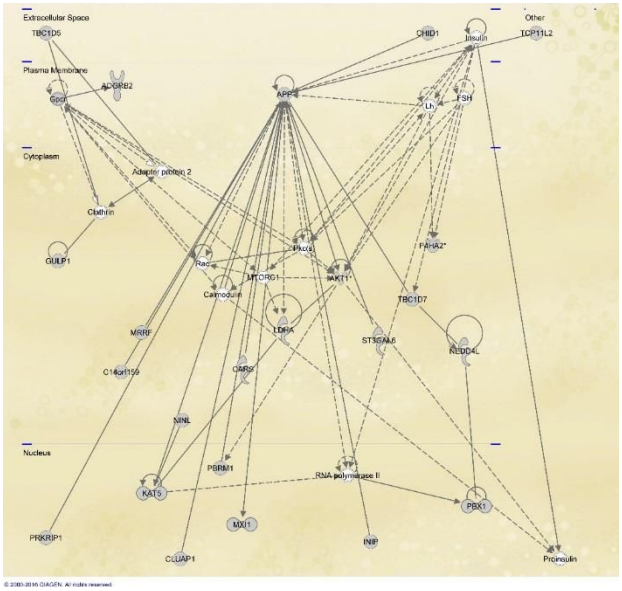

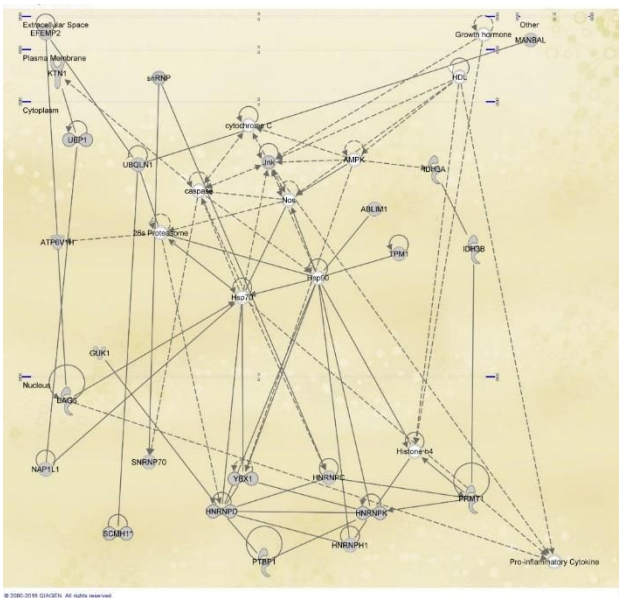

Supplementary Figure 3. IPA® network analysis of genes different for exon skipping in OGFOD1-KO vs. WT cardiomyocytes. Depicted in the left panel is the number 1 hit network indicated as “Cell death and survival, cell morphology, cell cycle”. Genes highlighted in grey showed significant differences for exon skipping events in OGFOD1-KO vs. WT identified by MISO analysis. Depicted in the right panel is the number 2 hit network indicated as “RNA post transcriptional modification, carbohydrate metabolism, nucleic acid metabolism”. Genes highlighted in grey showed significant differences for exon skipping events in OGFOD1-KO vs. WT identified by MISO analysis.

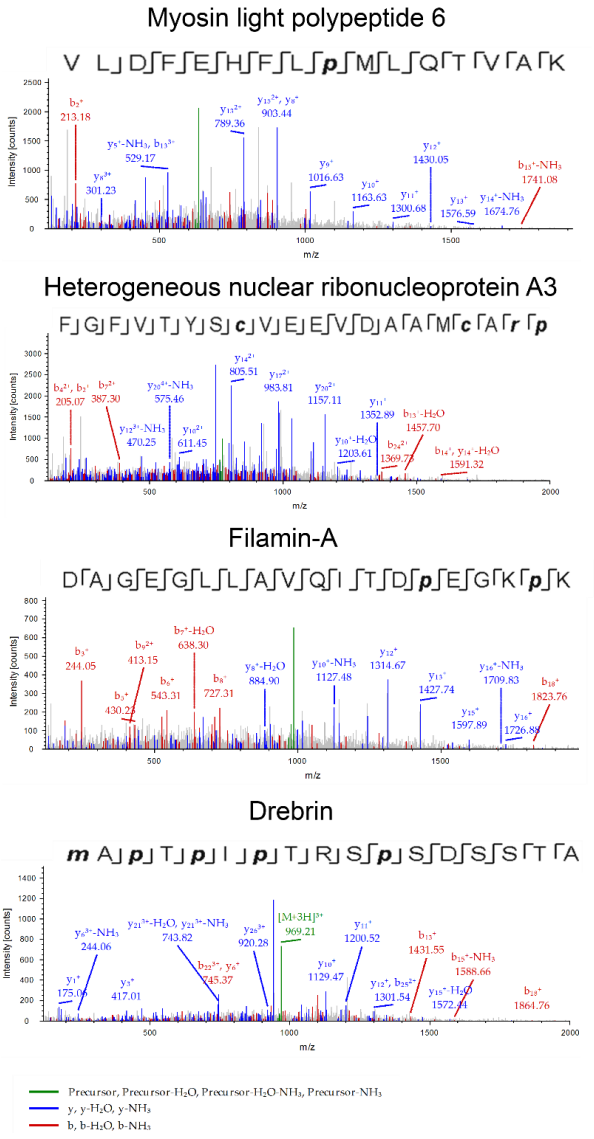

Supplementary Figure 4. Representative spectra for prolyl hydroxylated peptides identified in the proteomics experiment. Identification of prolyl hydroxylated peptides using mass spectrometry analysis of the pulse-chase labelled amino acids in human iPSC-CM. The mass-spectrometric data from the Orbitrap Fusion system was searched for proline oxidation in WT (n=3) and KO (n=3) samples at 3 independent time points (6h, 18h, 24h), respectively. Proteome Discoverer Software (PD, version 1.4) was used to filter the data for high peptide confidence (FDR of <1%), to identify prolyl oxidated peptides and for annotation to the respective proteins. Prolyl hydroxylated peptides were identified in at least 2/6 WT samples.

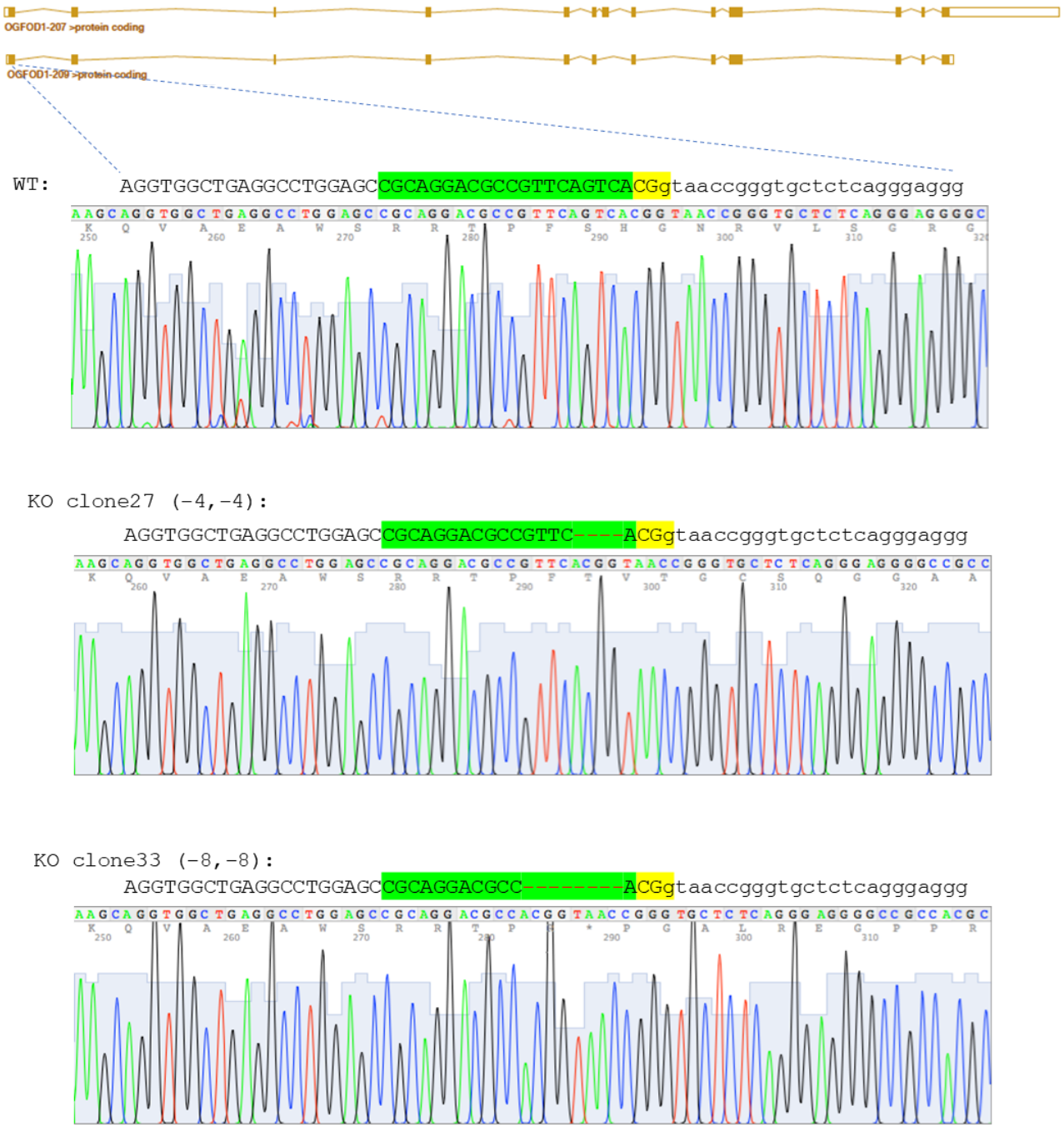

Supplementary Figure 5. Exon1 CDS of OGFOD1 is shared among all transcript variants, therefore was selected for gene knockout design of a gRNA (highlighted in green followed by PAM sequence in yellow) targeting 3'-end of Exon1. Single-cell clone 27 and clone 33 were confirmed by genomic PCR and Sanger sequencing to have bi-allelic frame-shift mutations,

(-4,-4) and (-8,-8), respectively, which resulted in pre-mature stop-codons and loss of OGFOD1 protein.

Biological Process	Enrichment Score	P-Value
Upregulated in KO		
GO:0006120~mitochondrial electron transport, NADH to ubiquinone	20.52	3.875405420018146E-17
GO:0006123~mitochondrial electron transport, cytochrome c to oxygen	6.72	1.3636530386906767E-8
GO:0006754~ATP biosynthetic process	5.39	8.23497879914469E-9
GO:0055010~ventricular cardiac muscle tissue morphogenesis	3.37	9.759931878085785E-4
GO:0035023~regulation of Rho protein signal transduction	2.92	4.3062773536352907E-4
GO:0016339~calcium-dependent cell-cell adhesion via plasma membrane cell adhesion molecules	2.68	0.0024262967839906273
GO:0048008~platelet-derived growth factor receptor signaling pathway	2.42	0.011497283621984695
GO:0055003~cardiac myofibril assembly	2.17	0.006788232714573066
GO:0006122~mitochondrial electron transport, ubiquinol to cytochrome c	2.11	0.003822866138711306
GO:0000188~inactivation of MAPK activity	2.02	0.004328449182627776
Downregulated in KO		
GO:0006614~SRP-dependent cotranslational protein targeting to membrane	4.81	1.3046591884013374E-10
GO:0055114~oxidation-reduction process	3.57	1.8811873795757778E-4
GO:0048791~calcium ion-regulated exocytosis of neurotransmitter	3.16	7.283076185734266E-4
GO:0018105~peptidyl-serine phosphorylation	2.63	0.057720210967139474
GO:0007156~homophilic cell adhesion via plasma membrane adhesion molecules	2.53	5.045740442125852E-4
GO:0042384~cilium assembly	2.49	0.00442387577198777
GO:1903779~regulation of cardiac conduction	2.07	0.08526646498092358
GO:0006687~glycosphingolipid metabolic process	2.00	0.008546983923751084

Supplemental Table 1. Transcriptomic changes in OGFOD1-KO vs. WT. Gene ontology analyses were performed with DAVID for enriched biological processes.